Chinese Chemical Letters 36 (2025) 110180

Contents lists available at ScienceDirect

Chinese Chemical Letters

journal homepage: www.elsevier.com/locate/cclet

A "spore-like" oral nanodrug delivery platform for precision targeted therapy of inflammatory bowel disease

Junfei Yang[a,b], Ke Wang[a,b], Shuxin Sun[a,b], Tianqi Pei[a,b], Junxiu Li[a,b], Xunwei Gong[a,b], Cuixia Zheng[c], Yun Zhang[a,b], Qingling Song[a,b,*], Lei Wang[a,b,*]

[a] School of Pharmaceutical Sciences, Zhengzhou University, Zhengzhou 450001, China
[b] Henan Key Laboratory of Targeting Therapy and Diagnosis for Critical Diseases, Zhengzhou 450001, China
[c] Henan University, Huaihe Hospital, Translational Medicine Center, Kaifeng 475000, China

ARTICLE INFO

Article history:
Received 9 April 2024
Revised 23 June 2024
Accepted 26 June 2024
Available online 26 June 2024

Keywords:
Gastrointestinal barrier
Spore-like
Precision targeted therapy
Spore coat
Gut microbiota

ABSTRACT

Colon-targeted oral drug delivery systems are one of the most promising therapeutic strategies for alleviating and curing inflammatory bowel disease (IBD), but they still face challenges in successfully passing through the harsh gastrointestinal environment and intestinal mucus barrier. To overcome the gastrointestinal barriers for oral drug delivery mentioned above, a "spore-like" oral nanodrug delivery platform (Cur/COS/SC NPs) has been developed. Firstly, chitooligosaccharides (COS) are encapsulated on the surface of Curcumin nanoparticles (Cur NPs) to form carrier-free nanoparticles (Cur/COS NPs). Subsequently, inspired by the natural high resistance of spore coat (SC), SC is chosen as the "protective umbrella" to encapsulate Cur/COS NPs for precision targeted therapy of IBD. After oral administration, SC can effectively protect NPs through the rugged gastrointestinal environment and exhibit excellent intestinal mucus penetration characteristics. Moreover, the negatively-charged Cur/COS/SC NPs specifically target positively-charged inflamed colon *via* electrostatic interactions. It is demonstrated that Cur/COS/SC NPs can promote the expression of tight junction proteins, inhibit aberrant activation of the Toll-like receptor 4/myeloid differentiation primary response gene 88/nuclear factor-κB (TLR4/MyD88/NF-κB) signaling pathway, and downregulate the levels of pro-inflammatory factors, exhibiting excellent anti-inflammatory effects. Notably, it is found that Cur/COS/SC NPs can significantly increase the richness and diversity of gut microbiota, and restore the homeostasis of gut microbiota by inhibiting pathogenic bacteria and promoting probiotics. Hence, Cur/COS/SC NPs provide a safe, efficient, and feasible new strategy for IBD treatment.

Inflammatory bowel disease (IBD) is a refractory chronic disease characterized by impaired intestinal barrier function, aberrant activation of inflammatory signaling pathways, and gut microbiota dysbiosis [1-3]. Its long-term recurrence can cause serious lesions, such as colon cancer [4,5]. Current clinical regimens for the treatment of IBD mainly focus on treating symptoms, but such treatment strategies are difficult to solve intestinal barrier damage and gut microbiota dysbiosis. Besides, conventional anti-IBD drugs (including 5-aminosalicylic acid, immunosuppressants) have limited bioavailability and may cause severe side effects due to their nonspecific anti-inflammatory properties [2,6,7]. Therefore, there is an urgent need for safe and effective comprehensive therapeutic strategies for IBD. Oral delivery is a highly preferred route of administration due to its patients' compliance and convenience. Additionally, with the flourishing of targeted drug delivery, colon targeted oral drug delivery systems can localize treatment to the inflamed colon, reducing side effects caused by systemic drug exposure, and gradually becoming an ideal treatment strategy for IBD [8,9]. For example, Zhang *et al.* developed cell membrane-coated nanoparticles for effective drug delivery. By camouflaging nanomaterials with a layer of the natural cell membrane, the obtained nanoparticles not only preserve the functionalities of the inner core particle but also acquire the unique colon targeting ability [10]. Wang *et al.* have constructed a mannose-modified liposome for macrophage targeting to improve therapeutic efficiency of colitis [11]. Unfortunately, the harsh gastrointestinal environment and mucus barrier pose several challenges to colon targeted oral drug delivery systems [12,13]. Therefore, developing a new targeted strategy to overcome the gastrointestinal barriers is urgently needed.

The gut microbiota is usually considered a metabolic organ of the body, and the symbiotic relationship between gut microbiota

* Corresponding authors.
E-mail addresses: songqingling@zzu.edu.cn (Q. Song), wanglei1@zzu.edu.cn (L. Wang).

https://doi.org/10.1016/j.cclet.2024.110180
1001-8417/

and host not only provides nutrients and a favorable metabolic environment for the microbiota but also facilitates the host's access to nutrients [14,15]. In addition, the dysbiosis of gut microbiota plays a key pathogenic role in IBD by altering the composition of gut microbiota and its metabolome [16-18]. In recent years, probiotic-based microecological preparations have been shown to positively regulate gut microbiota, reduce inflammatory responses, and improve the intestinal pathological microenvironment, which may become a breakthrough in clinical IBD treatment [19,20]. Notably, probiotic spore preparations are widely used as adjuvant treatments for many gastrointestinal diseases due to their strong resistance in the stomach, including *Bacillus coagulans* (BC) and *Bacillus subtilis* [21,22]. However, this strategy still has limitations in precision targeted therapy of IBD due to the fact that the germination of spores cannot be well controlled [23]. Interestingly, spore coat (SC) is the main component of spores that can resist harsh gastrointestinal conditions. Therefore, we isolated SC *in vitro* as the "protective umbrella" for the delivery of oral drugs in the gastrointestinal tract (GIT). Furthermore, after successfully passing through the stomach, negatively-charged SC can achieve targeted delivery and effective therapy within the positively-charged inflamed colon. Additionally, since SC originates from spores, we speculate that SC also has the potential to regulate the gut microbiota.

Curcumin (Cur) is an active polyphenol extracted from turmeric, which possesses excellent anti-inflammatory and immunomodulatory properties, while also regulating the gut microbiota [24-26]. It is a promising drug for the treatment of IBD. In certain instances, Cur has been synthesized in the form of nanoscale particles, referred to as Cur nanoparticles (Cur NPs). These nanoparticles are characterized by their outstanding biocompatibility and high therapeutic efficacy [27,28]. Unfortunately, the stability of pure drug NPs is poor, leading to suboptimal therapeutic efficacy. Interestingly, chitooligosaccharides (COS) are natural oligosaccharides with good solubility and biocompatibility. It not only has excellent anti-inflammatory and antioxidant activities but also exhibits prebiotic potential as an active factor for gut probiotics [29-31]. Thus, we encapsulate COS on the surface of Cur NPs *via* electrostatic adsorption to improve the stability of Cur NPs, and COS and Cur NPs cooperate to regulate gut microbiota.

Based on the importance of the intestinal pathological microenvironment and gut microbiota in the development of IBD, we designed a "spore-like" oral nanodrug delivery platform (Cur/COS/SC NPs) with an acid-resistant shell for precision targeted therapy of IBD (Scheme 1). This nanoplatform is for highly efficient IBD therapy by improving the intestinal pathological microenvironment and restoring gut microbiota homeostasis. Firstly, we extracted SC from the BC spores as the "protective umbrella" for drug delivery. After oral administration, Cur/COS/SC NPs were protected from the destruction of the gastric acid environment. Then Cur/COS/SC NPs were transported to the intestinal, where negatively-charged Cur/COS/SC NPs could be adsorbed onto the positively-charged inflamed colon *via* electrostatic interactions. Interestingly, Cur/COS/SC NPs showed good mucus permeability, which might be attributed to the composition of sulfhydryl groups in SC. Additionally, we further explored the specific mechanisms of Cur/COS/SC NPs to improve the colitis mice, including repairing intestinal barrier function, suppressing excessive activation of Toll-like receptor 4/myeloid differentiation primary response gene 88/nuclear factor-κB (TLR 4/MyD88/NF-κB) signaling pathway, and regulating gut microbiota homeostasis. In summary, Cur/COS/SC NPs could safely and effectively improve the pathological microenvironment of IBD from multiple perspectives, possessing extraordinary therapeutic advantages for IBD.

BC is a well-known probiotic widely utilized as adjunctive therapy for gastrointestinal diseases [32]. Spores are dormant structures of probiotics, highly resistant to gastric acid and can germinate to vegetative cells in the intestine microenvironment. SC enables spores to resist harsh environments and colonize in suitable areas [23]. Therefore, we plan to extract BC SC *in vitro* as the "protective umbrella" for NPs. Firstly, BC was cultured in a sporulation medium to separate BC spores. The morphology of BC and BC spores was according to transmission electron microscopy (TEM). As shown in Fig. S1 (Supporting information), the sizes of BC and BS spores were about 2–4 and 1–2 μm, respectively, and both were uniformly rod-shaped. These results confirmed the successful cultivation of BC and isolation of BC spores. Subsequently, BC spores were disrupted by ultrasonic and followed by gradient centrifugation to obtain SC. As shown in Fig. S2 (Supporting information), the phenomenon of SC isolating from spores was observed, indicating the successful preparation of SC.

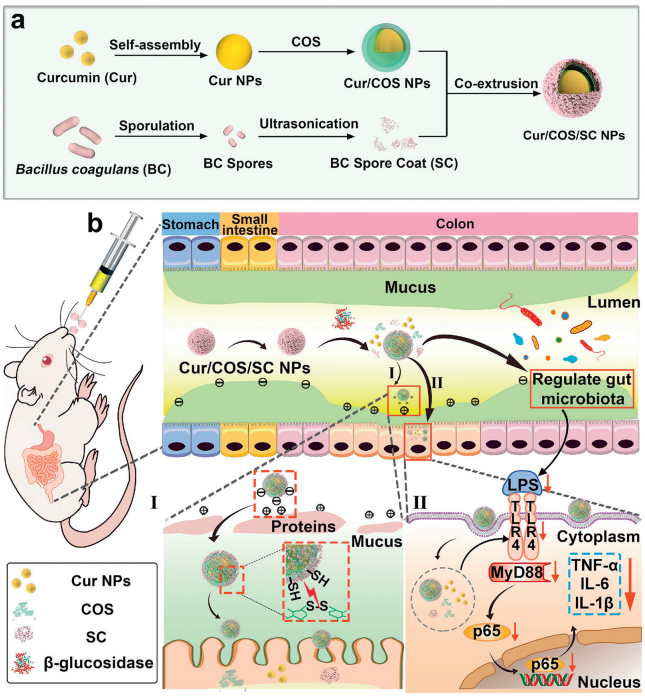

Scheme 1. Schematic diagram of fabrication and oral delivery mechanism of the "spore-like" nanoplatform. (a) Process of preparing Cur/COS/SC NPs. (b) The mechanism of Cur/COS/SC NPs for IBD treatment.

Cur is a hydrophobic compound with various pharmacological effects, including anti-inflammatory, antioxidant, anticancer, and gut microbiota modulation [24-26]. The preparation of Cur into Cur NPs improved the bioavailability and therapeutic efficacy of Cur [27]. As expected, Cur NPs showed a regular spherical shape (Fig. 1a). Then, Cur NPs were coated with COS *via* electrostatic adsorption to prepare Cur/COS NPs. Finally, the mixture of Cur/COS NPs and SC was passed through a liposome extruder to encapsulate SC on the surface of Cur/COS NPs to prepare Cur/COS/SC NPs. As shown in TEM images, compared with the smooth edges of unmodified Cur NPs, the coated Cur/COS NPs and Cur/COS/SC NPs showed obvious additional shells (Fig. 1a). In addition, dynamic light scattering (DLS) analysis demonstrated that the size and zeta potential of NPs changed after coating. The size of Cur NPs was about 49.06 ± 5.6 nm, while the size of Cur/COS NPs and Cur/COS/SC NPs were about 69.82 ± 6.0 and 91.12 ± 4.4 nm, respectively (Fig. 1b and Fig. S3a in Supporting information). Putting it all together, these results demonstrated the successful preparation of Cur NPs, Cur/COS NPs, and Cur/COS/SC NPs. To ensure that Cur/COS/SC NPs can effectively target inflamed colon, the negative charge of SC should be retained after wrapping around the surface of Cur/COS NPs. These negatively-charged NPs can specifically tar-

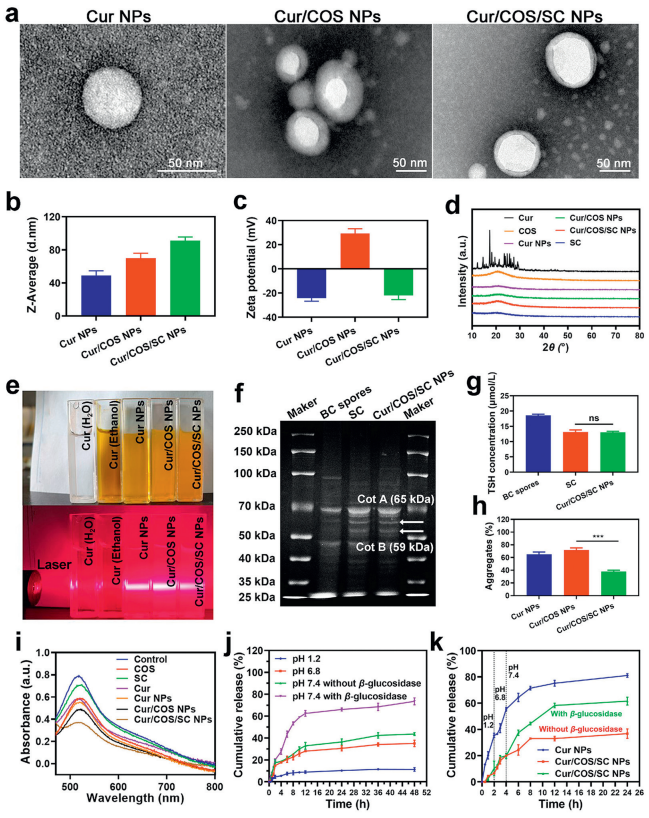

Fig. 1. Preparation and characterization of Cur/COS/SC NPs. (a) The TEM images of Cur NPs, Cur/COS NPs, and Cur/COS/SC NPs. Size b) and Zeta potential c) of different NPs. (d) XRD spectra. (e) Tyndall effect of different preparations. (f) Gel imaging. (g) The content of sulfhydryl groups. (h) The percentage of NPs-mucin aggregation. (i) DPPH radical scavenging assay. (j) Drug release behavior from Cur/COS/SC NPs at different pHs. (k) Release behavior of drugs from Cur NPs and Cur/COS/SC NPs incubated in a buffer solution with gradually varying pH for 24 h. Data are represented as means ± SD ($n = 3$), statistical analysis by one-way analysis of variance (ANOVA). $^{***}P < 0.001$. ns, no significance.

get inflamed colon *via* electrostatic interactions, characterized by an enrichment of positively-charged proteins [33,34]. As expected, the zeta potentials of Cur NPs, Cur/COS NPs, and Cur/COS/SC NPs were −24.2 ± 2.5, 29.3 ± 3.9, and −21.9 ± 3.6 mV, respectively (Fig. 1c and Fig. S3b in Supporting information). Considering that SC is essential for the spore to resist harsh environments, we speculated that SC could effectively protect NPs from the harsh gastric acid environment. To verify our conjecture, TEM was employed to evaluate the stability of Cur/COS/SC NPs by the morphology integrity after incubation with simulated gastric fluid and bile salts. As shown in Fig. S4 (Supporting information), Cur/COS/SC NPs still maintained the integrity of their shape after being incubated with simulated gastric fluid and bile salts. Furthermore, compared to other NPs, Cur/COS/SC NPs showed remarkable stability, with little change in solution dispersion and particle size over 7 days (Fig. S5 in Supporting information). Moreover, the X-ray diffraction (XRD) pattern of Cur showed multiple peaks owing to its crystallographic nature. In contrast, Cur NPs, Cur/COS NPs, and Cur/COS/SC NPs exhibited only one weak crystallization peak, indicating the successful preparation of NPs (Fig. 1d). Then, the ultraviolet–visible (UV–vis) spectrum confirmed the successful preparation of Cur/COS/SC NPs with an absorption peak of Cur (Fig. S6 in Supporting information), in which the loading capacity of Cur was 12.5%. The Tyndall effect is the scattering of light as a light beam passes through a colloid, commonly used as a preliminary validation of NPs formation [35]. As shown in Fig. 1e, under laser irradiation, the solutions of Cur NPs, Cur/COS NPs, and Cur/COS/SC NPs displayed significant Tyndall light scattering phenomena. In summary, these results demonstrated the successful preparation of Cur/COS/SC NPs.

Subsequently, the result of gel electrophoresis showed that the protein composition of Cur/COS/SC NPs was similar to SC, including Cot A (known for resistance) and Cot B (known for natural affinity), suggesting that SC was successfully wrapped on the surface of Cur/COS NPs (Fig. 1f) [36]. Additionally, to further investigate the function of SC, we analyzed the protein component of SC using liquid chromatography tandem mass spectrometry (LC/MS/MS). Multiple proteins were detected, such as domain proteins that enable spores to resist harsh environments and proteins with sulfhydryl groups on the surface that help penetrate intestinal mucus (Table S1 in Supporting information). The intestinal mucus barrier protects the epithelium from pathogenic microorganisms and harmful substances, but it may also reduce the absorption of drugs by intestinal epithelial cells, thereby decreasing the efficacy of drugs [37]. The sulfhydryl groups on the surface of SC can disrupt the disulfide bonds between mucin glycoproteins, promoting NPs to penetrate intestinal mucus [38]. As expected, the levels of sulfhydryl groups in SC and Cur/COS/SC NPs were comparable (Fig. 1g). In addition, compared with the other groups, Cur/COS/SC NPs had the lowest aggregate of 38% ± 2.1% (Fig. 1h). These results suggested that Cur/COS/SC NPs can escape mucus entrapment effectively.

Interestingly, we found that Cur/COS/SC NPs can scavenge DPPH radicals, indicating their excellent antioxidant capacity (Fig. 1i). Next, the controlled drug release behaviour of Cur/COS/SC NPs was detected under different simulated physiological conditions. We immersed Cur/COS/SC NPs in simulated gastric fluid (pH 1.2), intestinal fluid (pH 6.8), and colonic fluid (pH 7.4, with or without β-glycosidase). At pH 1.2, pH 6.8, and pH 7.4 without β-glycosidase, the cumulative release percentages of Cur were 11.31% ± 1.7%, 35.12% ± 2.91%, and 43.65% ± 1.29%, respectively. In contrast, at pH 7.4 with β-glycosidase, more than 70% of Cur was released because COS was degraded by the colon-specific β-glycosidase (Fig. 1j). Furthermore, after incubating Cur/COS/SC NPs with simulated colonic fluid for a period of time, the shell of Cur/COS/SC NPs showed significant rupture (Fig. S7 in Supporting information). These results demonstrated the enzyme-responsive drug release properties of Cur/COS/SC NPs. Subsequently, the programmed drug release properties were performed in a gradually pH-changing medium simulating the conditions of different parts of GIT. As shown in Fig. 1k, unprotected Cur NPs showed advanced release in the GIT, while the programmed release of Cur/COS/SC NPs reached 61.56% ± 2.96% under the specific pH and enzyme conditions in the colon environment.

The cytotoxicity of different formulations in Caco-2 cells was evaluated at 24 and 48 h. MTT results showed that the cell survival of Cur/COS/SC NPs (higher than 75%) at both 24 and 48 h was significantly higher than other three groups, indicating the exceptional biocompatibility of the Cur/COS/SC NPs (Fig. S8 in Supporting information). Efficient cellular uptake plays a crucial role in the therapeutic efficacy of NPs. To analyze the uptake efficiency of Cur/COS/SC NPs, Caco-2 cells were treated with Cur/COS/SC NPs for 0.5, 1, 2, and 4 h, respectively. Subsequently, cellular uptake was evaluated using flow cytometry and fluorescent microscopy, respectively. As shown in Fig. 2a and Fig. S9 (Supporting information), the fluorescence intensity gradually increased with the incubation time of Cur/COS/SC NPs, confirming that Cur/COS/SC NPs can be effectively uptaken by Caco-2 cells. Subsequently, intracellular behavior of NPs was tracked. As shown in Fig. S10 (Supporting information), there was a significant overlap between green fluorescence signals (Cur NPs) and red fluorescence signals (lysosomes), indicating that Cur NPs were swallowed by lysosomes. Nevertheless, the green fluorescence of Cur/COS/SC NPs separated from red fluorescence, suggesting that Cur/COS/SC NPs could be

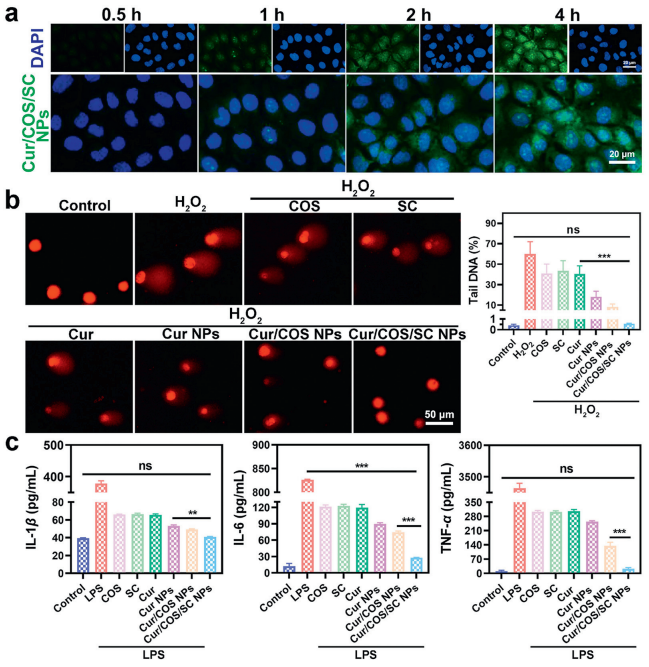

Fig. 2. Studies of cytotoxicity assay, cellular uptake assay and *in vitro* anti-inflammatory assay. (a) Cell uptake efficiency evaluated by fluorescent microscopy. Scale bar: 20 μm. (b) Comet assay and percentage of tail DNA. Scale bar: 50 μm. (c) Cytokines levels of IL-1β, IL-6, and TNF-α. Data are represented as means ± SD (n = 3), statistical analysis by one-way ANOVA. $^{**}P < 0.01$, $^{***}P < 0.001$.

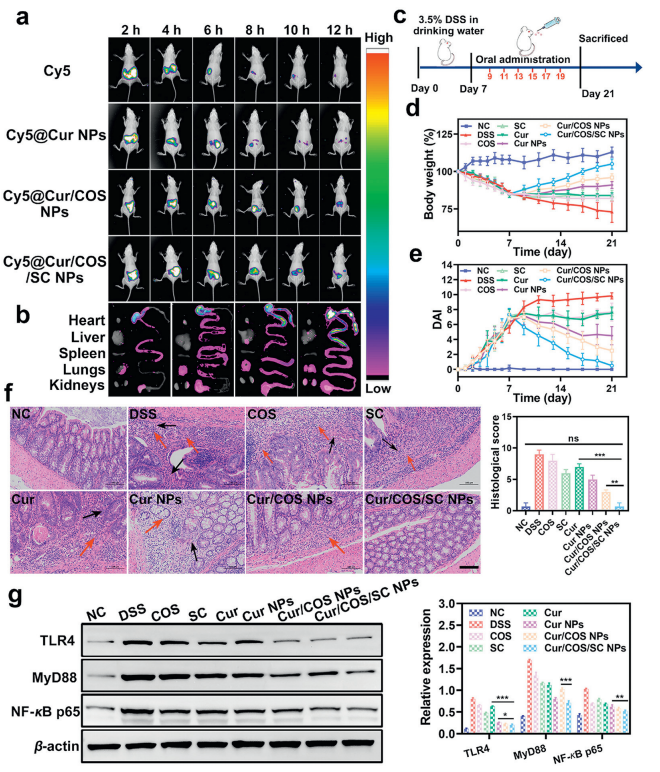

Fig. 3. Cur/COS/SC NPs exert a powerful therapeutic effect in DSS-induced colitis. (a) *In vivo* fluorescence images of colitis mice at the indicated time points after oral administration of different formulations. (b) The fluorescence images of major organs and colon tissues that were collected from mice after oral administration of different formulations for 12 h. (c) Schematic diagram of colitis model construction and treatment effect evaluation. (d) Daily body weight change of mice over 21 days. (e) DAI scores of mice in different groups. (f) H&E staining images and histology score of colon tissue. Scale bar: 100 μm. (g) Western blot analysis of TLR4, MyD88, and NF-κB. Data are represented as means ± SD (n = 3), statistical analysis by one-way ANOVA. $^{*}P < 0.05$, $^{**}P < 0.01$, $^{***}P < 0.001$.

uptaken by cells and escape from lysosomes with 4 h. Probably, the α-helix structures of the SC preferentially embed themselves in the phospholipid bilayer of biological membranes, where they interact to form pores for transmembrane activity [39]. This induces membrane fusion allowing endocytosis and lysis [40,41], and eventually facilitating lysosomal escape of NPs containing α-helix.

Reactive oxygen species (ROS) are byproducts of cellular oxidative metabolism. Physiological normal levels of ROS regulate cell proliferation and invasion, while excessive ROS can lead to oxidative stress and induce DNA damage [42]. Subsequently, the comet assay can be used for the measurement of oxidative DNA damage. As shown in Fig. 2b, H_2O_2 showed an obvious trailing phenomenon, indicating that H_2O_2-induced DNA damage in Caco-2 cells. In comparison, the trailing phenomenon of Cur/COS/SC NPs was not significant. These results indicated that Cur/COS/SC NPs could efficiently prevent H_2O_2-induced oxidative damage to cellular DNA.

After that, the anti-inflammatory properties of different formulations were detected. The levels of pro-inflammatory cytokines interleukin-1β (IL-1β), IL-6, and tumor necrosis factor-α (TNF-α) in lipopolysaccharide (LPS)-induced RAW264.7 cells were measured to determine the anti-inflammatory activity of each formulation. As shown in Fig. 2c, the levels of pro-inflammatory cytokines in Cur/COS/SC NPs group were substantially diminished, confirming the good anti-inflammatory efficacy of Cur/COS/SC NPs.

All animal experiments were approved by the Ethics Committee of Zhengzhou University. All animal experiments were carried out in strict accordance with the "Guidelines for the Feeding and Use of Laboratory Animals" which was required by the Ministry of Science and Technology of China. All BALB/c mice (15–20 g) were obtained from SPF Biotechnology Co., Ltd. (Beijing, China).

To determine whether Cur/COS/SC NPs can effectively target inflamed colon tissue, Cy5 labeled nanoplatforms (Cy5@NPs) were used for fluorescence tracking. The fluorescence of Cy5 and Cy5@NPs were significantly accumulated at the GIT sites in mice after being administrated for 2–4 h After 12 h administration, it could be observed that Cy5@Cur/COS/SC NPs showed strong fluorescence in the colon compared to other treatment groups (Figs. 3a and b, and Fig. S11 in Supporting information). In addition, we assessed the absorption effect of colonic epithelial cells on each formulation. Cur/COS/SC NPs displayed strong fluorescence in colonic epithelial cells, while the other three groups showed weak fluorescence (Fig. S12 in Supporting information). Therefore, Cur/COS/SC NPs could successfully target inflamed colon and be absorbed by colonic epithelial cells effectively.

Afterwards, the results of routine blood tests, renal and hepatic function tests showed no significant differences in various indicators between Cur/COS/SC NPs treated mice and healthy mice, confirming the good biocompatibility of Cur/COS/SC NPs (Fig. S13 in Supporting information). Furthermore, hematoxylin and eosin (H&E) staining of major tissues and organs showed negligible damage for all preparations, further indicating the biosafety of different preparations (Fig. S14 in Supporting information).

The anti-inflammatory effects of Cur/COS/SC NPs were further investigated in dextran sodium sulfate (DSS)-induced colitis mice. After being treated with 3.5% DSS for one week to induce colitis, mice were randomly divided into eight groups and treated with different formulations every other day for two weeks (Fig. 3c). At the end of treatment, mice were sacrificed and their colons were harvested for follow-up studies. Notably, the length of colon in Cur/COS/SC NPs group was similar to that in healthy mice, and significantly longer in comparison to other treatment groups

(Fig. S15 in Supporting information). Additionally, residual blood stools were observed in DSS group mice, which significantly improved after treatment with Cur/COS/SC NPs (Fig. S16 in Supporting information). Similarly, the increasing trend of body weight was obvious in Cur/COS/SC NPs group, while the other treatment groups failed to prevent weight loss (Fig. 3d). The severity of DSS-induced colitis was measured using the disease activity index (DAI), which assigned scores based on weight loss, stool consistency, and stool bleeding (Table S2 in Supporting information). As shown in Fig. 3e, the DAI of DSS group increased rapidly during the treatment process. However, the increased DAI was dramatically suppressed after treatment with Cur/COS/SC NPs, indicating that Cur/COS/SC NPs were effective in alleviating the severity of colitis. Moreover, the H&E staining images of colon tissue showed that, except for Cur/COS/SC NPs and normal control (NC) groups, the other treatment groups showed varying degrees of pathological damage such as inflammatory cell infiltration (red arrow) and loss of colonic glands and goblet cells (black arrow) (Fig. 3f and Table S3 in Supporting information). Zonula occluden-1 (ZO-1) and occludin, the tight junction-associated proteins that play essential roles in improving intestinal barrier function and maintaining intestinal homeostasis [43]. Immunofluorescence staining images showed that the expression levels of ZO-1 and Occludin in colon tissue were normalized after oral administration of Cur/COS/SC NPs (Fig. S17 in Supporting information). In conclusion, all these results demonstrated that Cur/COS/SC NPs have a significantly greater anti-inflammatory effect in colitis mice compared to other treatment groups.

TLR4 is a mediator between immune response and gut microbiota, playing a significant role in maintaining intestinal homeostasis. TLR4/MyD88/NF-κB signaling pathway is aberrant activation in DSS-induced colitis mice, which could further increase the generation of pro-inflammatory cytokines in the colon [3,44]. Therefore, inhibiting excessive activation of TLR4/MyD88/NF-κB signaling pathway has become a potentially effective strategy for treating IBD. The levels of TLR4, MyD88, and NF-κB proteins in colon tissue were determined by Western blot and immunofluorescence analysis. As expected, compared to other treatment groups, Cur/COS/SC NPs evidently suppressed the TLR4/MyD88/NF-κB signaling pathway, which was also verified by immunofluorescence (Fig. 3g and Fig. S19 in Supporting information). In addition, the level of myeloperoxidase (MPO) was dramatically suppressed after Cur/COS/SC NPs treatment (Fig. S18 in Supporting information). LPS is the main component of the outer membrane of Gram-negative bacteria and can induce the release of pro-inflammatory cytokines through TLR4 [45,46]. It could be found that the increased LPS and pro-inflammatory cytokines (IL-1β, IL-6, and TNF-α) were significantly down-regulated by Cur/COS/SC NPs (Fig. S20 in Supporting information). The above results consistently indicated that Cur/COS/SC NPs could inhibit the development of colitis, providing a promising strategy for the treatment of IBD.

The gut microbiota consists of hundreds of microorganisms that play an important role in maintaining immunity and intestinal homeostasis. There is emerging evidence that gut microbiota plays a crucial role in the occurrence and development of colitis [17,47]. Therefore, we further investigated whether Cur/COS/SC NPs treat-

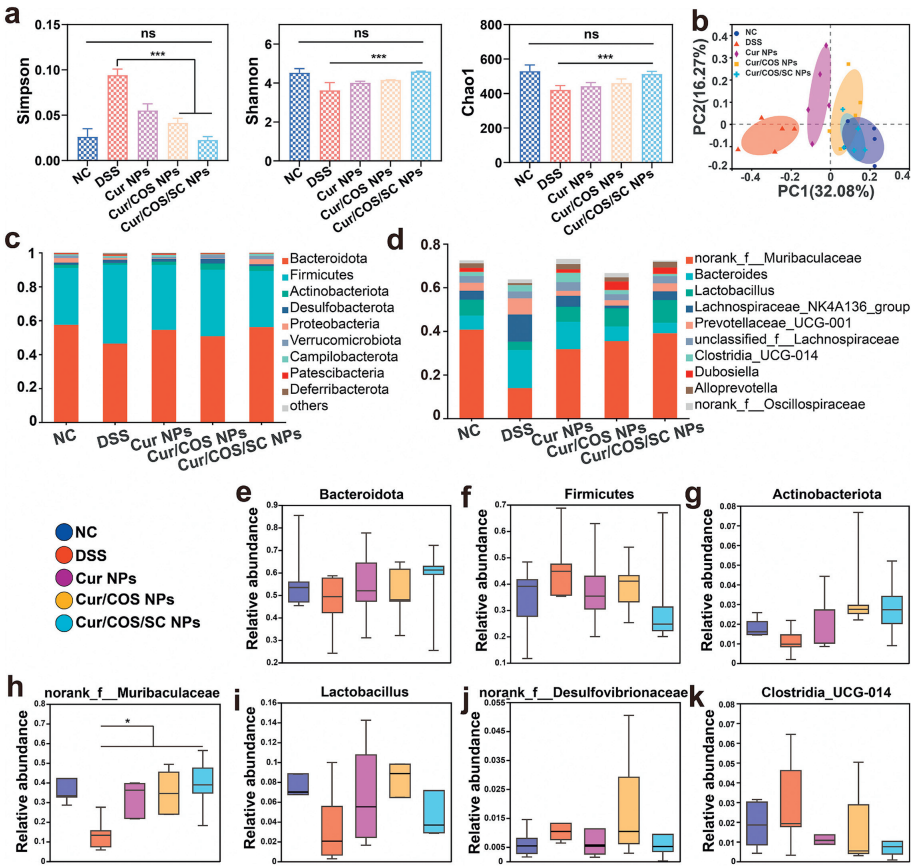

Fig. 4. The modulation of Cur/COS/SC NPs in the composition and abundance of gut microbiota. (a) The α-diversity of the gut microbiota, including Simpson, Shannon, and Chao1. (b) The β-diversity was shown by the PCoA plot. (c, d) The relative abundance of gut microbiota at the phylum and genus levels. (e–g) The relative abundance of *Bacteroidota*, *Firmicutes*, and *Actinobacteria* at the phylum level. (h–k) The relative abundance of *Muribaculaceae*, *Lactobacillus*, *Desulfovibrionaceae*, and *Clostridia_UCG-014* at the genus level. Data are represented as means ± SD ($n = 3$), statistical analysis by one-way ANOVA. $^{***}P < 0.001$.

ment could affect the progression of colitis by regulating the composition of gut microbiota in DSS-induced colitis mice. At the end of treatment, we collected the fecal of each colitis mouse and subsequently conducted structural differences analysis of the mice gut microbiota using 16 s rDNA gene sequencing technology. Previous studies have shown that the composition of gut microbiota decreases with the appearance of chronic diseases [48-50]. As expected, compared with other treatment groups, Cur/COS/SC NPs treatment significantly increased the α-diversity (Simpson, Shannon, and Chao1) of gut microbiota in DSS-induced mice (Fig. 4a). Further analysis of the Venn diagram revealed that Cur/COS/SC NPs treatment significantly increased the number of microbiotas (Fig. S21 in Supporting information). The principal coordinate analysis (PCoA) plot showed that gut microbiota of Cur/COS/SC NPs treatment group displayed a higher similarity to the healthy NC group compared to other treatment groups (Fig. 4b). These results suggested that Cur/COS/SC NPs showed promising potential to successfully restore microbiota homeostasis. Subsequently, the composition of the gut microbiota was assessed at the phylum and genus levels (Figs. 4c and d). At the phylum level, Cur/COS/SC NPs treatment significantly increased the proportion of probiotics, including *Bacteroidota* (known to improve inflammation and have beneficial effects on metabolic dysfunction) and *Actinobacteria* (known to maintain intestinal barrier homeostasis), while decreasing the proportion of *Firmicutes* (known to have pro-inflammatory properties) (Figs. 4e–g) [51-53]. In addition, it was further confirmed at the phylum level. As shown in Figs. 4h–k, Cur/COS/SC NPs treatment increased the relative abundance of *Muribaculaceae* and *Lactobacillus* but reduced the proportions of *Bacteroides* and *Clostridia_UCG-014*. *Muribaculaceae* is a typical probiotic that maintains homeostasis of intestinal barrier function while suppressing inflammation [54]. *Lactobacillus* is one of the most common probiotics and is commonly used as a food supplement to maintain health. However, *Desulfovibrionaceae* and *Clostridia_UCG-014* are both common pro-inflammatory bacteria [51,55]. These results indicated that Cur/COS/SC NPs can disrupt the ecological niche occupied by harmful bacteria and promote the proliferation of probiotics, which have a promising therapeutic against colitis.

To summarize, we constructed a "spore-like" oral nanodrug delivery platform (Cur/COS/SC NPs) that can overcome harsh gastrointestinal biological barriers for precision targeted therapy of IBD. This platform can achieve effective treatment for IBD by improving the pathological microenvironment of intestinal inflammation and restoring the gut microbiota homeostasis. With the camouflage of SC, the nanoparticles had advantages in several aspects, such as resistance to harsh gastric acid environment, good mucus permeability, precise targeting of the inflamed colon, and favorable biosafety. According to our results, Cur/COS/SC NPs exhibited excellent anti-inflammatory capacities, such as upregulating the expression of tight junction proteins, inhibiting abnormal activation of TLR4/MyD88/NF-κB signaling pathway, and suppressing the expression of inflammatory cytokines, demonstrating the excellent therapeutic effect of Cur/COS/SC NPs on colitis mice. Moreover, our results showed good efficacy of Cur/COS/SC NPs with few adverse effects in both *in vitro* and *in vivo* experiments. Significantly, the results of 16 s rDNA sequencing showed that Cur/COS/SC NPs could remarkably increase the richness and diversity of gut microbiota and restore the homeostasis of gut microbiota. In conclusion, this nanoplatform provides a prospective strategy for targeted oral drug delivery for IBD therapy.

Declaration of competing interest

The authors declare that they have no known competing financial interests or personal relationships that could have appeared to influence the work reported in this paper.

CRediT authorship contribution statement

Junfei Yang: Writing – review & editing, Writing – original draft, Software, Methodology, Investigation, Data curation. **Ke Wang:** Validation, Software, Methodology, Data curation. **Shuxin Sun:** Methodology, Investigation, Data curation. **Tianqi Pei:** Methodology, Investigation. **Junxiu Li:** Software, Methodology. **Xunwei Gong:** Software. **Cuixia Zheng:** Resources, Methodology. **Yun Zhang:** Writing – review & editing. **Qingling Song:** Writing – review & editing, Software. **Lei Wang:** Writing – review & editing, Supervision, Funding acquisition, Conceptualization.

Acknowledgments

This work was supported by the National Natural Science Foundation of China (Nos. 82272847, 82304417, 82303529, 82171333), China Postdoctoral Science Foundation (Nos. 2023TQ0307, 2023M743231, 2023M730971), Science and Technology Project of Henan Province (No. 242102311204), Postdoctoral Fellowship Program of CPSF (No. GZB20230675) and Modern Analysis and Computer Center of Zhengzhou University.

Supplementary materials

Supplementary material associated with this article can be found, in the online version, at doi:10.1016/j.cclet.2024.110180.

References

[1] A.T. Rahman, J. Shin, C.-H. Whang, et al., ACS Nano 17 (2023) 10996–11013.
[2] N.G. Kotla, Y. Rochev, Trends Mol. Med. 29 (2023) 241–253.
[3] C. Yu, D. Wang, Z. Yang, T. Wang, Int. J. Mol. Sci. 23 (2022) 6939.
[4] K. Rajamaki, A. Taira, R. Katainen, et al., Gastroenterol. 161 (2021) 592–607.
[5] L. Liang, R. Lin, Y. Xie, et al., Int. J. Biol. Sci. 17 (2021) 2548–2560.
[6] J.F. Colombel, P. Rutgeerts, W. Reinisch, et al., Gastroenterol. 141 (2011) 1194–1201.
[7] H.S. Sardo, F. Saremnejad, S. Bagheri, et al., Int. J. Pharm. 558 (2019) 367–379.
[8] H. Liu, Z. Cai, F. Wang, et al., Adv. Sci. 8 (2021) 2101619.
[9] D. Dehaini, R.H. Fang, L. Zhang, Bioeng. Transl. Med. 1 (2016) 30–46.
[10] J. Wang, H. Pan, J. Li, et al., Chin. Chem. Lett. 34 (2023) 107828.
[11] E. Wang, R. Han, M. Wu, et al., Chin. Chem. Lett. 35 (2024) 108361.
[12] Y. Xu, N. Shrestha, V. Preat, A. Beloqui, J. Control. Release 322 (2020) 486–508.
[13] A.M. dos Santos, S.G. Carvalho, A.B. Meneguin, et al., J. Control. Release 334 (2021) 353–366.
[14] S. Davoodi, E. Foley, Front. Immunol. 10 (2020) 3128.
[15] X. Zhu, K. Zhang, X. Teng, et al., Chem 9 (2023) 1094–1117.
[16] H. Gou, H. Su, D. Liu, et al., Gastroenterology 165 (2023) 1404–1419.
[17] R. Wu, R. Xiong, Y. Li, J. Chen, R. Yan, J. Autoimmun. 141 (2023) 103062.
[18] J. Ni, G.D. Wu, L. Albenberg, V.T. Tomov, Nat. Rev. Gastroenterol. Hepatol. 14 (2017) 573–584.
[19] M. Pesce, L. Seguella, A. Del Re, et al., Int. J. Mol. Sci. 23 (2022) 5466.
[20] H. Luo, G. Cao, C. Luo, et al., Pharmacol. Res. 178 (2022) 106146.
[21] Q. Song, H. Zhao, C. Zheng, et al., Adv. Funct. Mater. 31 (2021) 2104994.
[22] Q. Song, C. Zheng, J. Jia, et al., Adv. Mater. 31 (2019) 1903793.
[23] G. Christie, P. Setlow, Cell. Signalling 74 (2020) 109729.
[24] J. Yin, L. Wei, N. Wang, X. Li, M. Miao, J. Ethnopharmacol. 289 (2022) 115041.
[25] S.S. Kesharwani, R. Ahmad, M.A. Bakkari, et al., J. Controlled Release. 290 (2018) 165–179.
[26] J.D. Lewis, M.T. Abreu, Gastroenterol. 152 (2017) 398–414.
[27] J. Zhang, S. Li, F.-F. An, et al., Nanoscale 7 (2015) 13503–13510.
[28] Y. Wang, Y. Li, L. He, et al., Colloids Surf. B: Biointerfaces 203 (2021) 111756.
[29] W. Xia, P. Liu, J. Zhang, J. Chen, Food Hydrocoll. 25 (2011) 170–179.
[30] B. Zhu, H. He, D. Guo, M. Zhao, T. Hou, Food Hydrocoll. 102 (2020) 105567.
[31] X. Wei, L. Yu, C. Zhang, et al., Carbohydr. Polym. 299 (2023) 120156.
[32] Y. Wang, J. Lin, Z. Cheng, et al., Oxid. Med. Cell. Longevity. 2022 (2022) 5462390.
[33] S. Zhao, Y. Li, Q. Liu, et al., Adv. Funct. Mater. 30 (2020) 2004692.
[34] K. Wei, F. Gong, J. Wu, et al., ACS Nano 17 (2023) 21539–21552.
[35] X.Q. Sang, W.J. Yan, X.F. Qin, et al., Chin. J. Anal. Chem. 51 (2023) 100194.
[36] E. Ricca, S.M. Cutting, J. Nanobiotechnol. 1 (2003) 6.
[37] C.T. Nordgard, K.I. Draget, Adv. Drug Deliv. Rev. 124 (2018) 175–183.
[38] C. Menzel, A. Bernkop-Schnuerch, Adv. Drug Deliv. Rev. 124 (2018) 164–174.
[39] N.P. Gabrielson, H. Lu, L. Yin, et al., Angew. Chem. Int. Ed. 51 (2012) 1143–1147.
[40] H.X. Wang, Z. Song, Y.H. Lao, et al., Proc. Natl. Acad. Sci. U. S. A. 115 (2018) 4903–4908.
[41] F.J. Enguita, L.O. Martins, A.O. Henriques, M.A. Carrondo, J. Biol. Chem. 278 (2003) 19416–19425.

[42] P. Moller, D.M. Jensen, D.V. Christophersen, et al., Environ. Mol. Mutagen. 56 (2015) 97–110.
[43] W.T. Kuo, M.A. Odenwald, J.R. Turner, L. Zuo, Ann. NY Acad. Sci. 1514 (2022) 21–33.
[44] X. Mao, R. Sun, Q. Wang, et al., Front. Immunol. 12 (2022) 817583.
[45] N. Ma, D. Ma, X. Liu, et al., Environ. Int. 175 (2023) 107949.
[46] Y.C. Lu, W.C. Yeh, P.S. Ohashi, Cytokine 42 (2008) 145–151.
[47] A. Lavelle, H. Sokol, Nat. Rev. Gastro. Hepat. 17 (2020) 223–237.
[48] B. Chassaing, A.T. Gewirtz, Toxicol. Pathol. 42 (2014) 49–53.
[49] H. Sokol, S. Jegou, C. McQuitty, et al., Gut Microbes 9 (2018) 55–60.
[50] L. Mei, J. Guo, R. He, et al., Small 19 (2023) 202301129.
[51] B. Zhang, X. Fan, H. Du, et al., ACS Nano 17 (2023) 6081–6094.
[52] C. Binda, L.R. Lopetuso, G. Rizzatti, et al., Digest. Liver Dis. 50 (2018) 421–428.
[53] T. Magrone, E. Jirillo, Immun. Ageing 10 (2013) 31.
[54] X. Zhong, Y. Zhao, L. Huang, et al., Front. Microbiol. 14 (2023) 1140498.
[55] Y. Wang, X. Nan, Y. Zhao, et al., Microbiol. Spectrum. 9 (2021) e00105–e00121.